International Journal of Science, Environment
and Technology, Vol. 1, No 4, 2012, 285 - 301

RECYCLE OF WASTE FLY ASH: A RHEOLOGICAL INVESTIGATION

Monoj Sharma[1], Chandan Guria[1*], Ashis Sarkar[2] and Akhilendra K. Pathak[1]
[1]Department of Petroleum Engineering
[2]Department of Applied Chemistry,
Indian School of Mines, Dhanbad - 826 004, India
E-mail: cguria.che@gmail.com (*Corresponding Author*)

Abstract: This paper deals with the reduction of solid waste through recycling of fly ash for oil well drilling operation. For this, fly ash was grinded and classified into several fractions using float and sink test which will help to improve the polydispersity of waste fly ash. Float fractions of waste fly ash were analyzed for particle size and particle size distribution. Rheological studies were carried using this waste fly ash with varying particle size, particle size distribution and percent solid loading using Fann rotational viscometer. Wall share rates and shear stresses were calculated using Fann viscometer readings. Predicted wall shear rate and shear stress are used to calculate Herschel-Bulkley rheological model parameters for finding the shear rate dependent viscosities. Smaller particle size, narrow particle distribution and increased solid loading of classified fly ash will improve the suspension viscosity and will help to manipulate the rheological behaviour of the suspensions for efficient utilization. Finally, rheological results of fly ash suspensions were compared with aqueous bentonite clay suspensions to test the suitability of waste fly ash for oil well drilling application.
Keywords: Waste fly ash, recycling, float-sink test, rheology, rotational viscometer.

1. INTRODUCTION

Fly ash is a pozzolanic material, an admixture of several mineral oxides, and considered as a major environmental pollutant. Coal fired thermal power plants produces huge amount of fly ash and generates world's largest quantity of industrial solid wastes [1] and creates severe waste disposal problem. Utilization of fly ash is determined by their physical and chemical properties that include fineness, particle size, particle size distribution, specific surface area, particle shape, hardness, freeze-thaw resistance, and activity in aqueous suspension. Because of environmental problem, a good deal of work on the utilization of fly ash has been under taken worldwide. Utilization of fly ash as a resource material has been studied extensively in many areas such as extraction of valuable minerals, water pollution control, production of ceramic products, composite materials, agriculture, building materials, paint and plastic industries. Many investigators have also been carried out towards effective utilization of fly ash with understanding the potential environmental pollution and health impacts associated with the disposal of fly ash by land filling. Utilization of fly ash as a resource material has been studied extensively by many scientists and the details have been reviewed by Iyer and Scott [2] and Ahmaruzzaman [3].

In oil well drilling application, fly ash was mainly used for the stabilization of drilling fluid wastes to avoid ground water contamination [4, 5]. It was also used as a foamable drilling fluid for deep water offshore well operations [6]. Water based drilling mud typically contains clays, barite, lime, caustic soda and other chemicals. If the cuttings contain too much liquid, land disposal of these wastes raises groundwater pollution and difficult to reuse for construction purposes. Fly ash was usually used to reduce free water and toxic contaminants by solidification (which is also referred to as encapsulation, briquetting, fixation, and stabilization). Usually, hydration of the fly ash forms a crystalline structure, consisting of calcium-alumino-silicate which results a rock-like, monolithic and hardened mass [7]. High-calcium (Class-C) fly ash has the property of cementation and is very useful in stabilizing the drilling fluid. Mahlaba et al. [8, 9] studied the slurry behaviour of fly ash and brine suspension as backfill materials to conserve fresh water. Recently, Yang and Tang [10] studied the effectiveness of fly ash and polyacrylamide composite as a sand fixing agent for wind erosion control.

About 53.0 % of India's energy supply is based on coal and shall be so for few the next few decades [11]. There are about 82 coal fired thermal power stations producing approximately 130 million tonnes of fly ash per year in the Country [12]. Till date, nearly 38.0 % of fly ash has been successfully utilized in the Country at preset (reported by National Thermal Power Corporation, India) in various fields including land filling, cement making, concrete products making particularly bricks, blocks and tiles, road making, and mines backfilling. For efficient utilization of fly ash in different areas, it is essential to know the flow behaviour of waste fly ash slurry suspension with varying particle size, particle size distribution and particle loading.

Fann viscometer is a common apparatus for the measurement of rheological properties of drilling fluid suspensions [13-15]. It consists of two coaxial cylinders (called, rotor and bob) with drilling fluids being placed in the annulus between them. Dial reading of bob (in degree) is a measured of torque and is converted into shear stress quite accurately [15]. However, major problem arises in determining the bob shear rate which is not straight forward, and is a subject of research for long time. The difficulty of estimating the wall shear rate is mainly due to the non-uniform distribution of fluid flow in the concentric annulus. Numerous methods have been proposed in the recent past to determine the wall shear rate and the details have been reviewed in details by Wazer et al. [16], Steffe [17] and Estelle et al. [18]. Komoda et al. [19] proposed torque measurement technique to estimate the viscosity of gas solid suspensions using mono-disperse silica particles. Chandel et al. [20] also suggested a methodology to determine the rheological properties of highly concentrated coal ash slurry using Weissenberg Rheogoniometer. To estimate rheological properties of the drilling fluid, simplest Newtonian approximation has been used for given geometry of Fann Viscometer and is related to the rotation speed of rotor *only* [15]. Till date, this procedure is followed to determine apparent viscosity, plastic viscosity, Bingham yield point and gel strength of drilling fluids in the laboratory as well as in the field to monitor the performance of an oil well drilling [13-15].

In the present study, waste fly ash from thermal power plant has been tested for the application of oil well drilling to minimize solid waste disposal problem. For this, fly ash has been grinded using ball mill to reduce particle size. The grinded fly ash has been classified using float and sink test to improve the polydispersity of grinded fly ash. Classified fly ash has been analyzed for particle size and particle size distribution using laser beam particle size analyzer. Wall shear rates and shear stresses for different fly ash suspensions are calculated using Fann rotational viscometer reading. Herschel-Bulkley rheological model parameters are calculated for finding the shear rate dependent viscosities. Effects of particle size, particle size distribution and percent solid loading of fly ash on rheology have also been carried out to manipulate the flow behaviour of waste fly ash suspensions. Finally, the rheological properties of the classified waste fly ash suspensions are compared with aqueous bentonite suspensions (commonly used clay to maintain the desired viscosity of drilling fluid) with varying solid loading to check the suitability of classified waste fly ash as a drilling fluid additive.

2 EXPERIMENTAL

2.1 *Materials and Method*

Virgin fly ash was collected from thermal power plant (Rihand, Noida, India: Field No. 08) with the following specifications: specific gravity range 2.0-2.5, and particle size range 10-100 μm. Chemical assay of virgin fly ash was determined using X-ray

Fluorescence (Model: PW-1710; Make: Philips) with following composition (wt %): SiO_2-59.23, Al_2O_3-32.16, Fe_2O_3-5.03, CaO-0.9 and TiO_2-2.59. Morphological analysis of virgin fly ash using Scanning Electron Microscope (Model S-440, LEO) was carried out and the microphotograph is shown in Fig. 1. It reveals that fly ash particles are spherical and smooth. Zinc chloride (SD Fine-Chem Ltd., Mumbai, India) with specific gravity: 2.91, and assay: 99.9 % was used as a medium for float and sink tests. Bentonite clay powder (SD Fine-Chem Ltd., Mumbai, India) was directly used for rheological analysis with the following specifications: loss on drying: 3.0 %, and pH: 10.0 (4.0 g in 200 ml water). Underground raw water (total hardness: 680.0 mg/l and total dissolved solids: 955.0 mg/l) was used to prepare the aqueous suspensions fly ash and bentonite.

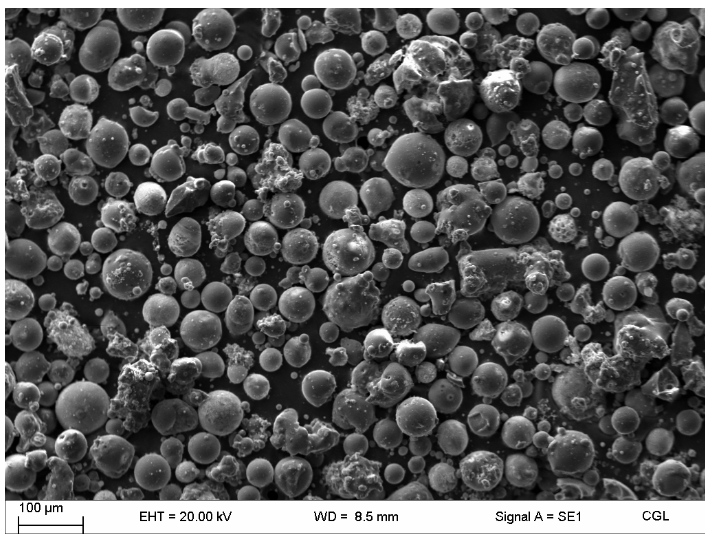

Fig. 1 Scanning Electron Microscope microphotograph of virgin fly ash.

2.2 *Classification of Virgin Fly Ash*

Virgin fly ash was sieved using 200 mesh sieve to reject naturally occurring fines and grinded using laboratory scale ball mill (capacity: 500 g) for 24 hours to reduce particle size. Float and sink tests were carried out for the classification of grinded fly ash to improve the polydispersity. Aqueous zinc chloride solutions with 1.5, 1.8 and 2.0 specific gravity is used as floating medium to carry out the above tests. To prepare above specific gravity solutions, solid zinc chloride of 188.0 g, 265.0 g and 358.0 g were taken and dissolved in 100 cc of distilled water respectively. Desired quantity of grinded fly ash was mixed thoroughly with aqueous zinc chloride solutions with varying specific gravities. Floats were collected from the top and found to be 0.28, 0.35 and 0.40 g dry float/g virgin dry fly ash using 1.5, 1.8 and 2.0 specific gravity zinc chloride solution respectively. Time required for settling the waste fly ash was found to be 10-12 minutes. Collected floats were thoroughly mixed with distilled water and separated using centrifuge. The process was repeated to remove the residual amount of zinc chloride present in fly ash float. These washed floats without residual zinc chloride (called classified fly ash float) were dried in an oven at 100^{o}C for 48 hours. This dried classified fly ash floats were then used for rheological studies.

2.3 *Particle Size Distribution of Classified Fly Ash*

Virgin fly ash and classified fly ash float samples were analysed for particle size and particle size distribution. The size analysis was carried out using a laser beam particle size analyzer (Mastersizer S Ver. 2.19, Malvern Instruments Ltd., Malvern, U.K.) that measures particle sizes between 0.001 to 1000 μm. Here, laser beam was passed through an aqueous suspension of dispersed particles and angle of diffraction was measured. Angle of diffraction increases as particle size reduces. Following details are used for analysis: range lens - 300 mm, beam length - 2.4 mm, presentation - 3RHD, particle refractive index - (1.9285, 0.1000), dispersant refractive index - 1.3300, analysis model-polydisperse, and distribution type-volume, and particle specific gravity - 2.18. Differential distribution along with cumulative distribution for oversize and undersize virgin and classified fly ash float samples are shown in Figs. 2a-2d and corresponding particle size distribution for these fly ash samples was given in Table 1.

3. EVALUATION OF WALL SHEAR RATE AND SHEAR STRESS MODEL

Laboratory Fann viscometer with six rotational speeds (*API* RP 13B: Model 35) is commonly used to measure rheological properties of the drilling fluids i.e., plastic viscosity, apparent viscosity, yield stress, initial gel strength and 10 minutes gel strength. In this viscometer, bob (inner cylinder) is stationary and rotor sleeve or cup (outer cylinder) rotates at a constant speed. Therefore, one can obtain the following equation to estimate wall share rate ($\dot{\gamma}_w$) for Fann rotational viscometer (details are given in Appendix A)

$$\dot{\gamma}_w = \frac{2\pi N}{60}\left[\frac{\acute{n}+2}{\acute{n}}\right] \tag{1}$$

where $\acute{n} = \frac{dln\tau_w}{dln\omega_2}$ is the flow behaviour index of the rotating fluid.

Wall share rate in above equation depends on the rotational speed (N) of rotor and the flow

Table 1 Particle size distribution statistics for virgin and classified fly ash float samples

Description	Virgin fly ash (sp. gr. 2.2)	Classified fly ash: floating medium sp. gr. 1.5	Classified fly ash: floating medium sp. gr. 1.8	Classified fly ash: floating medium sp. gr. 2.0
D 10[1] (μm)	4.85	1.26	1.25	1.17
D25 (μm)	10.25	2.99	2.62	2.08
D50[2] (μm)	18.22	4.72	5.62	16.92
D75 (μm)	29.54	8.47	11.01	3.795
D90[3] (μm)	45.61	14.47	22.8	16.92
Span[4]	2.237	3.834	2.799	0.931
Volume mean Diameter (μm)	11.42	10.39	8.95	8.0
Surface mean Diameter (μm)	3.25	3.21	2.99	2.75
Number mean Diameter (μm)	0.94	0.93	0.97	0.98

behaviour index ($\acute{n}$) of rotating fluid. Neglecting end effect at the bottom of the bob, shear stress at the inner wall (τ_w) is calculated from the torque applied on the bob [15]:

$$\tau_w = \frac{k\theta}{2\pi r_1^2 h} \tag{2}$$

where k, θ, r_1 and h are the spring constant, dial reading, bob radius and bob height of Fann viscometer respectively. Substituting standard configuration of viscometer (Model 35) i.e., bob radius (r_1) = 17.245 mm, rotor radius (r_2) = 18.415 mm, bob height (h) = 38.0 mm and spring constant (k) = 3.87×10^{-5} N.m/scale unit, one will able to evaluate Eqs. (1) and (2).

4 RESULTS AND DISCUSSION

Classified fly ash float samples were analysed for particle size analysis using laser beam particle size analyzer (Mastersizer S Ver. 2.19). Particle size distribution of virgin fly ash and classified fly ash floats are shown in Figs. 2a-2d and the details of the distribution statistics for these samples are given in Table 1. It is observed that the float obtained from the floating medium with highest specific gravity (i.e., 2.0) results the lowest particle size with lowest span value which is an indication of narrow particle size distribution with reduced polydispersity.

1 diameter of the particles below 10 % volume of under size cumulative distribution

2 diameter of the particles below 50 % volume of under size cumulative distribution

3 diameter of the particles below 90 % volume of under size cumulative distribution

4 span $= \frac{D90-D10}{D50}$, breadth of the particle size distribution

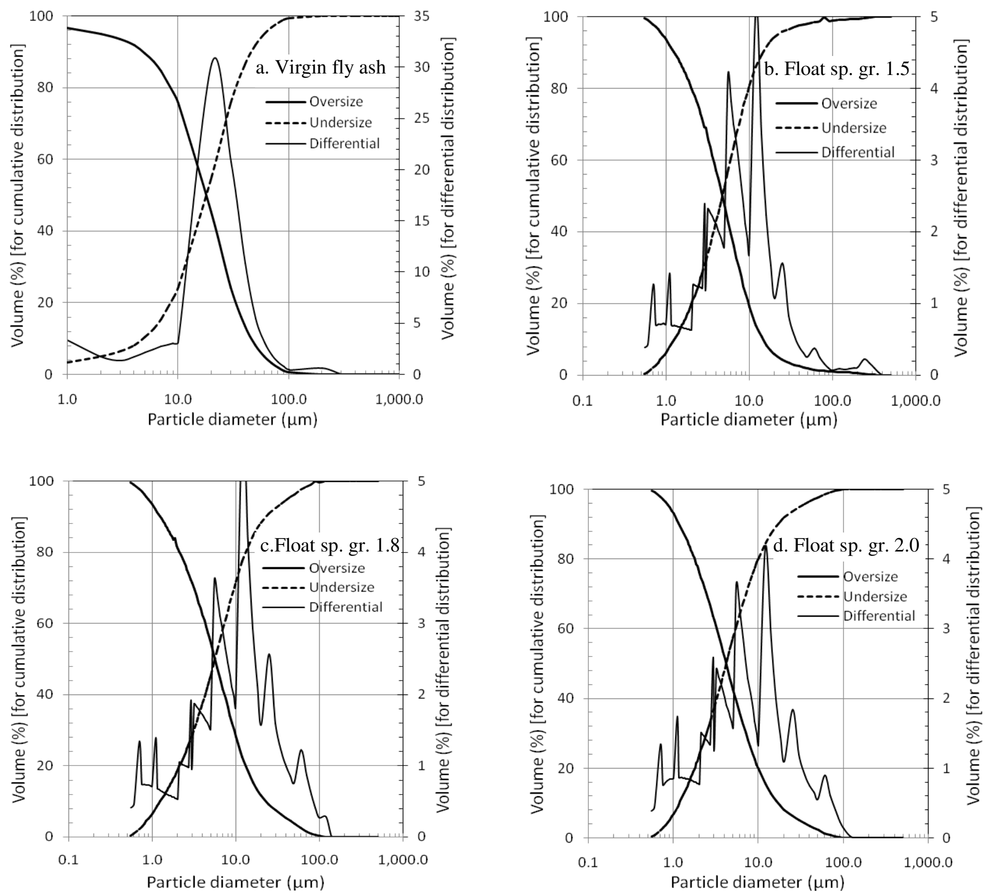

Fig. 2 Particle size distribution of virgin and classified fly ash floats with different specific gravities

Several rheological tests with different particle size, particle size distribution and solid loading were performed with aqueous suspension of classified fly ash float samples using Fann viscometer and *all* rheological results were compared with aqueous bentonite (a common additive for drilling fluid) suspensions with different solid loadings. Details of the experimental results using Fann viscometer i.e., dial reading (in degree) *vs*. rotational speed (in rpm) for bentonite and classified fly ash suspensions are shown in Figs. 3a-3d. It is observed that the dial reading at a given rotational speed gradually increases with the specific gravity of the float medium i.e., highest dial reading were obtained with lowest average particle size distribution. Now, Eqs. (1) and (2) are now used to calculate of shear rates at the bob wall using different rotational speeds (N) and dial readings (θ) of Fann viscometer. First, flow behaviour index $\acute{n} = \frac{dln\tau_w}{dln\omega_2}$ is calculated, and obtained from the

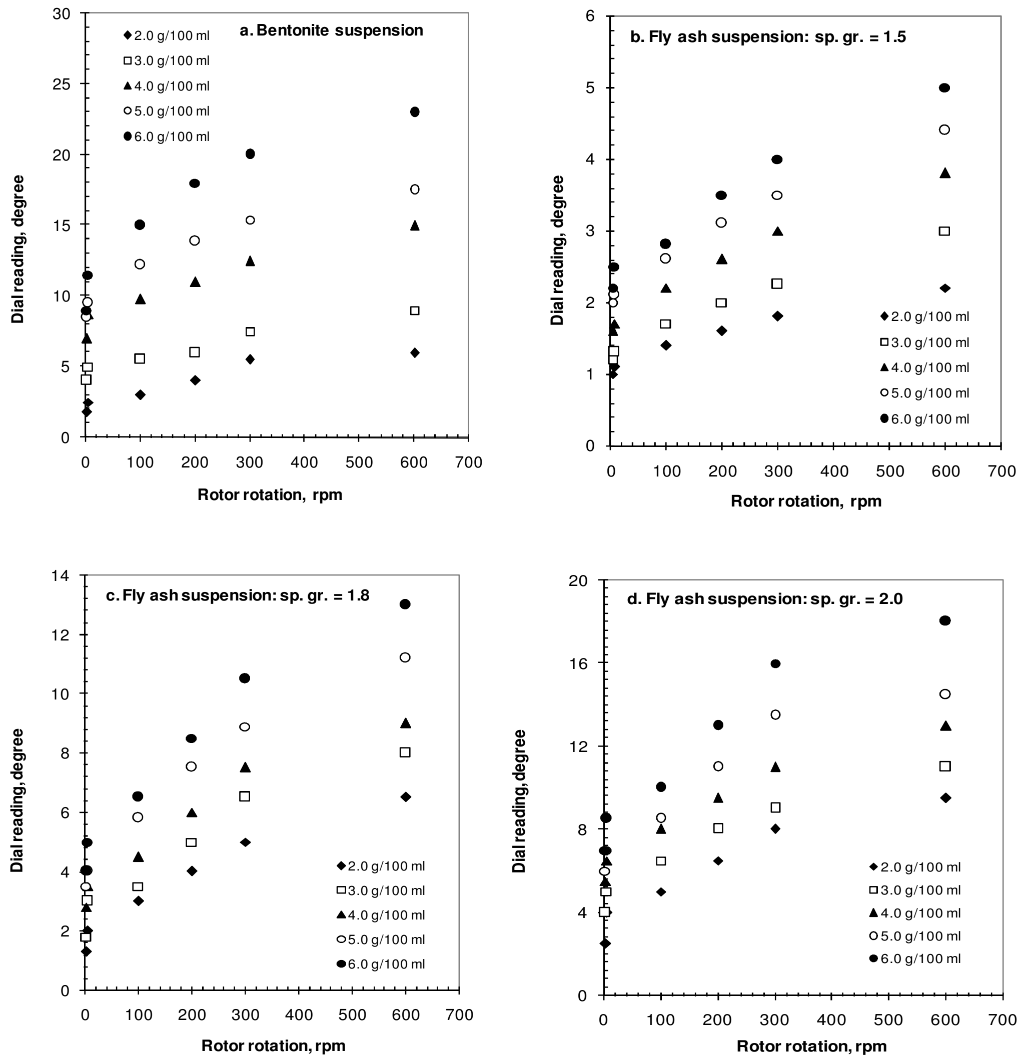

Fig. 3 Variation of Fann viscometer dial reading (θ) with rotor rotational speed (N) for bentonite and classified fly ash suspensions.

slope of wall shear stress at the bob (i.e., Eq. 2) *vs.* angular rotor velocity (i.e., $\omega_2 = \frac{2\pi N}{60}$) plots. The best fit equations are obtained from logarithmic plots of τ_w *vs.* ω_2 [i.e., $\ln \tau_w = a_0 + a_1 \ln \omega + a_2 (\ln \omega)^2$] and subsequent differentiation will result the flow behaviour index (i.e., $n' = \frac{d(\ln \tau_w)}{d(\ln \omega)} = a_1 + 2a_2 \ln \omega$) of the rotating fluid. Details of the best equation for aqueous bentonite and classified fly ash suspensions are reported in Table 2. It is noticed that the flow behaviour index has marked effect on rotational speed of rotor for given suspension and it gradually increases with the increase in rotational

Table 2 Flow behaviour index, $\acute{n}$, for bentonite and fly ash suspensions

% loading (g/100 ml raw water)	$\ln \tau_w = a_0 + a_1 \ln \omega + a_2 (\ln \omega)^2$ **a₀**	**a₁**	**a₂**	**R²**
Bentonite				
2	0.1114	0.1081	0.0342	0.97
3	0.8064	0.0330	0.0320	0.98
4	1.3912	0.0551	0.0223	0.99
5	1.5696	0.0819	0.0162	0.99
6	1.7274	0.1292	0.0110	0.98
Classified fly ash float suspension (*sp. gr. 1.5*)				
2	-0.6098	0.0555	0.0279	0.99
3	-0.4556	0.0417	0.0396	0.98
4	-0.1782	0.0390	0.0389	0.98
5	0.0278	0.0252	0.0389	0.98
6	0.1455	0.0168	0.0414	0.97
Classified fly ash float suspension (*sp. gr. 1.8*)				
2	-0.0864	0.1953	0.0261	0.97
3	0.2170	0.1421	0.0340	0.95
4	0.4928	0.0919	0.0386	0.97
5	0.6893	0.1013	0.0372	0.99
6	0.8483	0.0903	0.0390	0.97
Classified fly ash float suspension (*sp. gr. 2.0*)				
2	0.5657	0.1666	0.0174	0.96
3	0.8773	0.1063	0.0227	0.98
4	1.1387	0.0710	0.0263	0.98
5	1.2198	0.0759	0.0294	0.96
6	1.3798	0.0676	0.0337	0.97

speed. Using the flow behaviour index values (Table 2), wall shear rates ($\dot{\gamma}_w$) at different ω_2 are calculated using Eq. (1). Predicted wall shear rates and shear stresses for bentonite and classified fly ash suspensions with different particle size distributions and solid loadings are shown in Figs. 4a–4d. It is noted that the calculated wall shear stress for bentonite suspension increases with the solid loading for given particle size distribution (Fig. 4a). Similar to bentonite suspension, wall shear stress for classified fly ash float suspensions also increases with increase in solid loading (Figs. 4b-4d). It is interesting to note that the shear stress of classified fly as suspension increases with the decrease in particle size and its distribution (i.e. increases with the increase in specific gravity of floating medium) for a given fly ash solid loading (Figs. 4b-4d). In this case, increase in shear stress is mainly due to the increased number of particles in the suspension. It is also observed for bentonite suspension that the wall shear rate increases with solid loading for

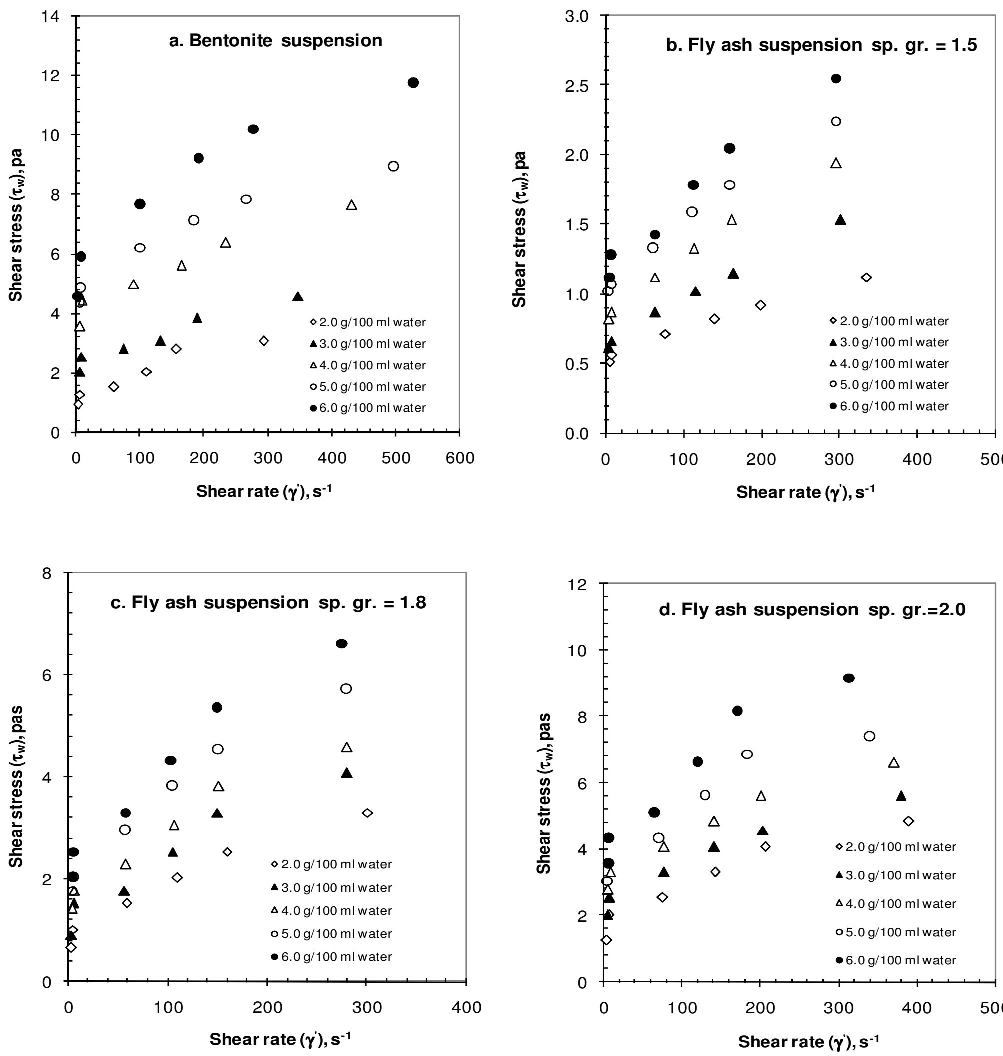

Fig. 4 Variation of wall shear stress at the bob (τ_w: Eq. 2) with wall shear rate at the bob ($\dot{\gamma}_w$: Eq. 1) for bentonite and classified fly ash suspensions.

a given rotational speed (e.g., 600 rpm: Fig. 4a) whereas shear rate for the classified fly ash suspensions are *almost* independent of solid loading at the same rotational speed (e.g., 600 rpm: Figs. 4b-4d). In the case of bentonite suspensions, wall shear rate (or relative rate of deformation) is higher than the fly ash suspensions for given solid loading which results the sufficient reduction in viscosity of bentonite suspensions at higher stress as compared to the fly ash suspensions. Therefore, pseudo plastic behaviour (i.e., shear rate of thinning) of bentonite suspension predominates over classified fly ash suspensions. The increased shear rate at given shear stress for bentonite suspensions is mainly due to the crystalline charged surface of bentonite particles [14] and these particles orient in the direction of the applied shear at the higher shear rates. In other words, increase in shear rate of bentonite loading is an indication of layered structured and improved surface properties. On the other hand, fly ash does not have such layer structures (Fig. 1) as compared to bentonite, and wall shear rates are *almost* unaffected by the fly ash loading (Figs. 4b-4d). Though the rheological properties of classified fly ash and bentonite suspension differ from each other, still classified fly ash may be used for oil well drilling after appropriate *surface modifications*.

Wall shear stress and wall shear rate plots (Figs. 4a–4d) are also used to determine the model parameters of Herschel-Bulkley (HB) rheological equation [21] to determine the dependence of share rate dependent plastic viscosities. For this, HB equation is transformed into the following convenient form:

$$ln(\tau_w - \tau_0) = lnK_{HB} + n_{HB} ln(\dot{\gamma}_w) \quad (3)$$

where, n_{HB} = Herschel-Bulkley flow behaviour index, K_{HB} = Herschel-Bulkley flow consistency parameter and τ_0 = true yield point.

Slope and intercept of $\ln(\tau_w - \tau_0)$ *vs*. $\ln(\dot{\gamma}_w)$ plots will result n_{HB} and K_{HB} respectively for *all* the suspensions. Here, τ_0 is obtained by extrapolation of individual shear stress *vs*. shear rate plot to the zero shear rate. Details of HB parameters of aqueous bentonite and classified fly ash suspension are shown in Table 3. Using HB rheological model, shear rate dependent plastic viscosity (η) is obtained and written as:

$$\eta = K\dot{\gamma}_w{}^{n_{HB}-1} \quad (4)$$

Logarithmic plastic viscosity (η) values are plotted against wall shear rates ($\dot{\gamma}_w$), and the results are shown in Figs. 5a–5d. It is observed that log plastic viscosity decreases rapidly with increase in shear rate, which is a typical behaviour of pseudo plastic fluid. It is also noted that pseudo plastic behaviour bentonite suspensions at high shear rates (Fig. 5a) is more sensitive than that of classified fly ash suspensions (Figs. 5b-5d). It is also noticed that plastic viscosity of fly ash suspensions with increases with the decrease in particle size (or increases with the increase in specific gravity of the floating medium) for given solid loading (Figs. 5b-5d). This is also due to the increased number of particles in the suspension causing more particle-particle interactions and leads to higher plastic viscosity. It is also observed that the variation of viscosity with share rate for the classified fly ash suspension using higher specific gravity floating medium (i.e., Specific gravity: 2.0) is very much close to the bentonite suspension. In other words, the rheological behaviour of the classified waste fly ash float is pretty similar to the bentonite suspensions. Therefore,

Table 3 Herschel-Bulkley parameters for bentonite and classified fly ash suspensions

% loading (g/100 cc raw water)	$\tau_w = \tau_0 + K\dot{\gamma}^n$			R^2
	τ_0	n	K	
Bentonite				
2	0.35	0.3165	0.4202	0.96
3	0.85	0.2283	0.8487	0.93
4	2.03	0.2500	1.0931	0.94
5	2.56	0.2674	1.1560	0.98
6	3.06	0.3228	1.1309	0.96
Classified fly ash float suspension (sp. gr. 1.5)				
2	0.41	0.4425	0.0485	0.97
3	0.49	0.4949	0.0536	0.98
4	0.70	0.5512	0.0491	0.98
5	0.90	0.5669	0.0484	0.97
6	0.99	0.5460	0.0617	0.95
Classified fly ash float suspension (sp. gr. 1.8)				
2	0.20	0.3595	0.3631	0.96
3	0.50	0.3980	0.3379	0.94
4	0.81	0.3813	0.4033	0.96
5	1.00	0.3918	0.4738	0.98
6	1.14	0.3796	0.5851	0.96
Classified fly ash float suspension (sp. gr. 2.0)				
2	0.83	0.3881	0.3821	0.94
3	1.30	0.3490	0.5066	0.96
4	1.93	0.3507	0.5450	0.96
5	2.14	0.3841	0.5472	0.95
6	2.18	0.3473	0.8851	0.94

waste fly ash may be used as a drilling fluid after processing as well as surface modification. It is also mentioned that one can manipulate rheological properties of classified fly ash suspension by varying particle size, particle size distribution and solid loading of classified waste fly ash float for efficient handling.

5 CONCLUSIONS

In this study, we have proposed the efficient utilization of waste fly ash as a drilling fluid for oil well drilling through processing and estimating rheological properties. For this, fly ash has been grinded and classified using float and sink test to improve the polydispersity. Aqueous zinc chloride solution is used as a floating medium for classification. Classified fly ash floats were analyzed for chemical assay, particle size and particle size distribution. High specific gravity floating medium improves polydispersity of waste fly ash as compared to low specific gravity floating medium. Wall share rates and

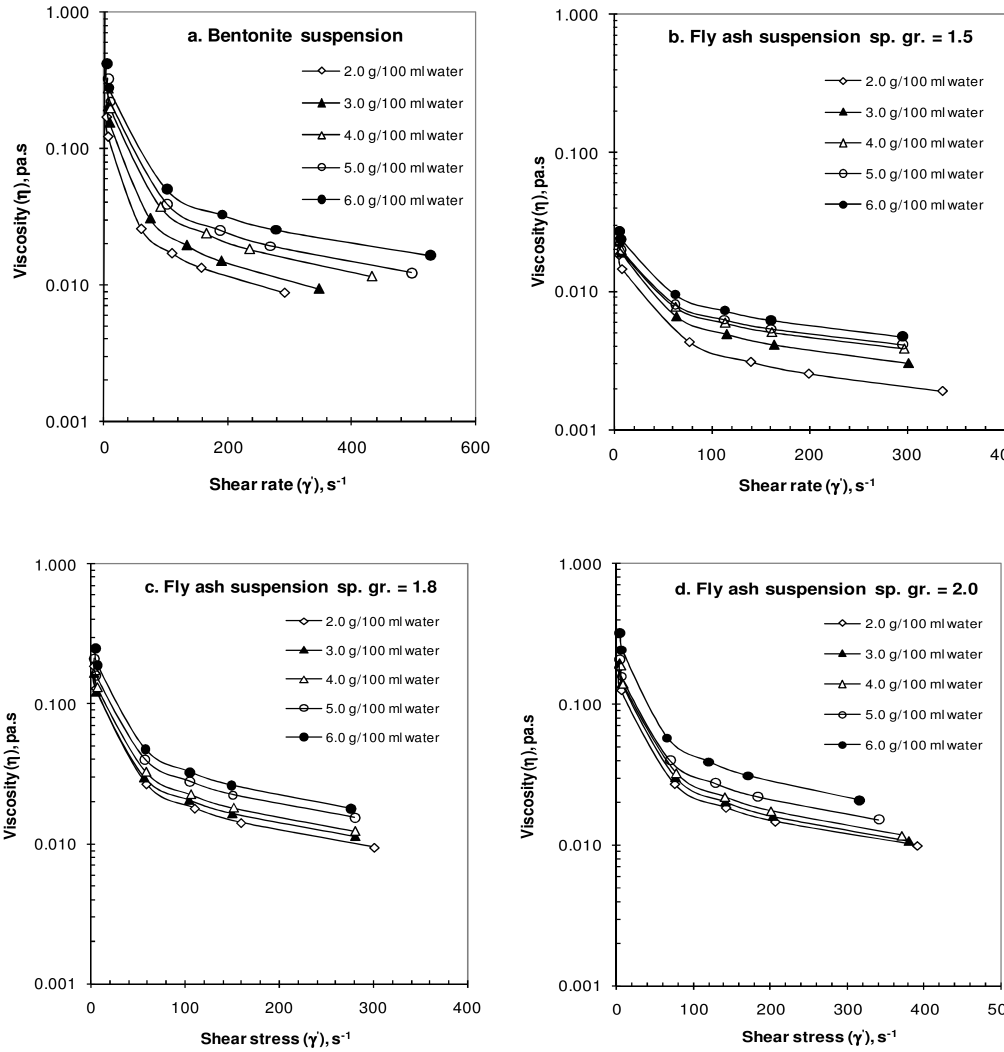

Fig. 5 Variation of plastic viscosity (η) with shear rate ($\dot{\gamma}_w$) for bentonite and classified fly ash suspensions.

share stresses of fly ash suspensions have been calculated using rotational Fann viscometer readings with varying particle size, particle distribution and percent solid loadings. Rheological results are compared with aqueous bentonite suspensions. Results show that bentonite suspensions exhibits high share rate of deformation than the fly ash suspension particularly at high shear stress. Calculated wall shear rates and shear stresses are fitted to Herschel-Bulkley rheological model to predict share rate dependent plastic viscosities with varying solid loadings, particle size and particle size distribution. Smaller particle size, narrow particle distribution and increased solid loading of classified fly ash float will improve plastic viscosity and rheological properties are very much closer to bentonite suspension. Though, the rheological properties of fly ash suspensions differ from bentonite suspension particularly at higher rates, but appropriate surface modification of fly ash may improve the rheological characteristics.

ACKNOWLEDGEMENTS

Partial financial support from Indian School of Mines, Dhanbad [through minor research project grant 2009/MRP/PE/Acad] is gratefully acknowledged. Help from Institute of Drilling Technology, Oil and Natural Gas Corporation, Dehradun, India for particle size analysis is gratefully acknowledged.

RFERENCES

[1] R. Giere, L.E. Carleton, G.R. Lumpkin, Micro- and nano-chemistry of fly ash from a coal-fired power plant, American Mineralogist, 88 (2003) 1853 - 1865.

[2] R.S. Iyer, J.A. Scott, Power station fly ash-a review of value-added utilization outside of the construction industry, Resources Conservation and Recycling, 31 (2001) 217 - 228.

[3] M. Ahmaruzzaman, A review on the utilization of fly ash, Progress in Energy and Combustion Science, 36 (2010) 327 - 363.

[4] G.M. Deeley, L.W. Laguros, Stabilization of drilling fluid waste with fly ash, Materials Research Society Symposium Proceedings, 86 (1987) 77-85.

[5] L.F. Thompsom, Drilling fluid waste minimization and stabilization using polymer technology, Paper No. SPE 29196, SPE Eastern Regional Meeting, Charleston, West Virginia, 1994.

[6] P.L. Totten, J.E. Griffth, B.L. King, Foamable drilling fluid, EP0761798, 1997. (http://www. freepatents-online.com/EP0761798.pdf).

[7] J.R. Conner, S.L.A. Hoeffner, Critical review of stabilization/solidification technology, Critical Reviews in Environmental Science and Technology, 28 (1998) 397 - 462.

[8] J.S. Mahlaba, E.P. Kearsley, R.A. Kruger, Effect of fly ash characteristics on the behaviour of pastes prepared under varied brine conditions, Minerals Engineering, 24 (2011a) 923 - 929.

[9] J.S. Mahlaba, E.P. Kearsley, R.A. Kruger, P.C. Pretorius, Evaluation of workability and strength development of fly ash pastes prepared with industrial brines rich in SO_4^{-2} and Cl^- to expand brine utilisation, Minerals Engineering, 24 (2011b) 1077 - 1081.

[10] K. Yang, Z. Tang, Effectiveness of fly ash and polyacrylamide as a sand-fixing agent for wind erosion control. Water Air & Soil Pollution (2012) DOI 10.1007/s11270-012-1173-x.

[11] C. Friedman, T. Schaffer, India's Energy Options: Coal and Beyond. South Asia Monitor, August, 132 (2009) 1 - 4.

[12] Y. Singh, Fly Ash utilization in India, available at http://www.wealthywaste.com/fly-ash-utilization-in-india (accessed on May 31st, 2011).

[13] C. Gatlin, Petroleum Engineering: Drilling and Well Completions, Prentice Hall, Inc., Englewood Cliffs, 1960.

[14] G.R. Gray, H.C.H. Darley, Composition and Properties of Drilling and Completion Fluids, 5th edn., Gulf Professional Publishing Company, Butterworth-Heinemann, 1981.

[15] A.T. Jr Bourgoyne, K.K. Millheim, M.E. Chenevert, F.S. Jr Young, Applied Drilling Engineering, SPE Text Book Series, Vol. 2, Richardson, TX, 1986.

[16] J.R. Wazer, J.W. Lyons, K.Y. Kim, R.E. Colwell, Viscosity and flow measurement. A laboratory handbook of rheology, Interscience publishers, New York, 1963.

[17] J.F. Steffe, Rheological Methods in Food Engineering Process, Freeman Press, East Lansing, MI, 1996.

[18] P. Estelle, L. Christophe, A. Perrot, Processing the Couette viscometry data using a Bingham approximation in shear rate calculation, Journal of Non-Newtonian Fluid Mechanics, 154 (2008) 31 - 38.

[19] Y. Komoda, K. Nakashima, H. Hiroshi, H. Hiromoto, Viscosity measuring technique for gas-solid suspensions, Advanced Powder Technology, 17 (2006) 333-343.

[20] S. Chandel, S.N. Singh, V. Seshadri, Deposition characteristics of coal ash slurries at higher concentrations, Advanced Powder Technology, 20 (2009) 383-389.

[21] W.H. Herschel, R. Bulkley, Konsistenzmessungen von Gummi-Benzollosungen, Kolloid Z, 39 (1926) 291 - 300.

[22] B. Bird, W. Stewart, E. Lightfoot, Transport Phenomena, 2nd ed,. John Wiley & Sons, New York, 2002.

[23] J.G. Savins, G.C. Wallick, M.R. Foster, The differentiation method in Rheology: III. Couette Flow, Society of petroleum Engineering Journal, March SPE 306 (1963) 14-18.

APPENDIX A: ESTIMATION OF WALL SHARE RATE USING FANN ROTATIONAL VISCOMETER

The generalized cylindrical θ-component equation of motion for this Fann viscometer under steady state condition is given by the following differential equation [22]:

$$\frac{1}{r^2}\frac{\partial}{\partial r}(r^2\tau_{r\theta}) = 0 \tag{A.1}$$

where $\tau_{r\theta}$ = θ-component momentum flux (i.e., shear stress) in the positive direction of *r*.

On integration, Eq. (A.1) reduces to

$$r^2\tau_{r\theta} = \text{constant} \tag{A.2}$$

Considering the slippage between two successive layers of fluid in the annular space of the viscometer, shear rate ($\dot{\gamma} = \frac{dv}{dr}$) is given by following equation [15]:

$$\dot{\gamma} = r\frac{d\omega}{dr} \tag{A.3}$$

Combining Eqs (A.2) and (A.3) will result the following differential equation:

$$d\omega = -\dot{\gamma}\frac{d\tau_{r\theta}}{2\tau_{r\theta}} \tag{A.4}$$

At steady state, the rotor sleeve is rotating at constant angular velocity (ω_2) and the bob is motionless (i.e., $\omega_1 = 0$). Integrating Eq. (A.4) within the limits, the following equation is obtained after omitting subscript $r\theta$:

$$\int_0^{\omega_2} d\omega = \omega_2 = -\frac{1}{2}\int_{\tau_{r1}}^{\tau_{r2}}\dot{\gamma}\frac{d\tau}{\tau} \tag{A.5}$$

where $\tau_{r1}$and τ_{r2} are the shear stresses at the bob and rotor wall respectively.

Equation (A.2) is applicable to any point in the annulus of the viscometer and is written as

$$\tau_{r2} = \frac{r_1^2}{r_2^2}\tau_{r1} \tag{A.6}$$

Now substituting upper limit of the integral in Eq. (A.5), i.e., τ_{r2} in terms of τ_{r1}using Eq. (A.6), one may obtain the following integral with modified limits i.e.,

$$\omega_2 = -\frac{1}{2}\int_{\tau_{r1}}^{\frac{r_1^2}{r_2^2}\tau_{r1}}\dot{\gamma}\frac{d\tau}{\tau} \tag{A.7}$$

Differentiating above equation with respect to τ_{r1}using Leibnitz formula, one may obtain the following simplified equation [23]:

$$\frac{d\omega_2}{d\tau_{r1}} = -\frac{1}{2}\left[\frac{\dot{\gamma}_{r2}}{\tau_{r2}}\frac{r_1^2}{r_2^2} - \frac{\dot{\gamma}_{r1}}{\tau_{r1}}\right] \tag{A.8}$$

where $\dot{\gamma}_{r1}$ and $\dot{\gamma}_{r2}$ are the shear rates at the bob and rotor wall respectively.

Now substituting Eq. (A.6), above equation (Eq. A.8) reduces to the following form:

$$\frac{d\omega_2}{d\tau_{r1}} = \frac{1}{2\tau_{r1}}[\dot{\gamma}_{r1} - \dot{\gamma}_{r2}] \tag{A.9}$$

In Fann viscometer, torque is transmitted from rotor sleeve to bob through viscous drag between two successive layers of the fluid. Since ω_2 is related to the rotation of the entire body, it is assumed that the layer of fluid just adjacent to the rotor sleeve is also moving with the same angular velocity of rotor sleeve (i.e., ω_2). This assumption is quite common [16, 17] and one may write $\dot{\gamma}_{r2} = \omega_2$ and replacing subscript r_1 by w, the wall share rate at the bob is given by the following equation:

$$\dot{\gamma}_w = \omega_2 + 2\tau_w \frac{d\omega_2}{d\tau_w} \qquad \text{(A.10)}$$

Above equation demonstrates the variation of wall shear rate ($\dot{\gamma}_w$) with angular velocity of the rotor sleeve (related to the rotor rpm, N) and wall shear stress (related to the bob dial reading, θ and Fann viscometer geometry), and is transformed into its convenient form i.e.,

$$\dot{\gamma}_w = \omega_2 + 2\omega_2 \frac{dln\omega_2}{dln\tau_w} \qquad \text{(A.11)}$$

Substituting, $\acute{n} = \frac{dln\tau_w}{dln\omega_2}$ (called flow behaviour index) and $\omega_2 = \frac{2\pi N}{60}$ in Eq. (A.11), one will obtain the following equation:

$$\dot{\gamma}_w = \frac{2\pi N}{60}\left[\frac{\acute{n}+2}{\acute{n}}\right] \qquad (1)$$

Therefore, Eqs. (1) and (2) will help to generate the consistency plots (i.e., shear stress *vs.* shear rate) for bentonite and classified waste fly ash aqueous suspensions.

*Received Aug 24, 2012 * Published Oct, 2012*